Load Flow Analysis and the Impact of a Solar PV Generator in a Radial Distribution Network

Mohamed Ali Zdiri
CEM Laboratory, Engineering School of Sfax, Tunisia
mohamed-ali.zdiri@enis.tn
(corresponding author)

Bilel Dhouib
CEM Laboratory, Engineering School of Sfax, Tunisia
dhouib.bilel@gmail.com

Zuhair Alaas
Department of Electrical Engineering, Faculty of Engineering, Jazan University, Saudi Arabia
zalaas@jazanu.edu.sa

Fatma Ben Salem
CEM Laboratory, Engineering School of Sfax, Tunisia
fatma_bs@yahoo.fr

Hsan Hadj Abdallah
CEM Laboratory, Engineering School of Sfax, Tunisia
hsan.hajabdallah@enis.tn

Received: 17 November 2022 | Revised: 10 December 2022 | Accepted: 18 December 2022

ABSTRACT

The distribution system acts as a conduit between the consumer and the bulk power grid. Due to characteristics such as a high resistance/reactance ratio, distribution networks cannot be solved using conventional methods, such as the Gauss-Seidel and Newton–Raphson. This research proposes a method for the calculation of the power flow in radial networks that considers their wide range of resistance and reactance values, PV generator characteristics, and radial structure. An iterative methodology is employed, with each iteration beginning with the branch that has the highest accurate power flow solution. The procedure is reliable and effective over various workloads and network configurations. To confirm the effectiveness of the suggested technique on the simple and IEEE 33-bus radial distribution system, simulations were carried out in MATLAB. The implications of including a renewable energy source, such as a PV generator, in the network under consideration are investigated by simulation result comparison. The optimal location of the PV generator was also determined using an Artificial Neural Network (ANN) controller. The results of the identification process improve the already exceptional efficacy and performance of the ANN controller.

Keywords-radial network; PV generator; power flow; identification; ANN controller; MATLAB

I. INTRODUCTION

Distribution systems operate as conduits between the bulk power grid and the customers. Primary or main feeders and lateral distributors are frequently used in the distribution circuits. The main feeder travels across the main load centers after leaving the substation. Radial distribution systems are referred to as lateral distributors because they join various load sites to the main feeder. The ease of use and low cost of radial systems result in their increasing popularity.

Power flow is an essential tool in power system analysis. The maximum currents carried by distribution feeders and the associated voltage dips, annual energy loss, and dependability of meeting consumer needs must all be considered in order to design properly the expansion and operation characteristics of distribution networks. Given that each optimization study

requires several power flow runs, the effectiveness of such an algorithm is crucial. However, the numerous inputs used as the foundation for these studies, including load forecast, load model coefficients, network parameters, and formation of bus shunts, are frequently estimated with a certain degree of error. Owing to practical challenges in data collection in large and complicated distribution systems, this uncertainty is typically non-statistical in nature.

Electric distribution networks have certain inherent characteristics, including:

- Radial or weakly mesh structures
- Unbalanced operation and unbalanced distributed loads
- High number of buses and branches
- Wide range of resistance and reactance values
- Operating in multiple phases

During the past two decades, the Newton–Raphson and rapidly decoupled power flow solution approaches and their variations, have successfully been utilized to solve "well-behaved" power systems [1, 2]. However, flaws have been noted when these algorithms have been extensively applied to faulty and improperly initialized power systems. The Gauss-Seidel power flow approach, another traditional power flow method, has proven to be incredibly ineffective when fixing large power systems while being quite durable. Distribution networks fall within the category of ill-conditioned power systems for the generic Newton–Raphson and rapid decoupled power flow algorithms due to their wide range of resistance and reactance values and radial structure. Furthermore, due to the development of renewable energy sources, the resolution of distribution systems should consider them [3]. To solve the distribution system problem, the load flow method must be modified.

Power flow is often separated into two categories. The first category, which suggests recursive solutions without recurring derivatives in their formulations, comprises power flow strategies that incorporate the distribution network graph simply by rearranging the power flow equations to obtain a recursive formula [4–9]. Iterative solutions based on linear approximations belong to the second class of approaches that use Taylor's series expansion of power flow equations in real and complex domains. Additionally, the use of Distributed Generation (DG) systems, which heavily rely on renewable energy, has become increasingly popular [10], and their development has rapidly advanced [11]. The installation of DG units at the distribution level has numerous advantages, such as reduced peak loads, enhanced system security, dependability, voltage stability, grid strengthening, cutting on-peak operating costs, and reduced network loss [12, 13].

To calculate power flow, fundamental radial network assumptions are considered in this study. This approach is comparable to others where an iterative procedure is used along the branches. Because it is based on a precise power flow solution for a single branch that provides a comprehensive solution, the essential concept is offered in the literature [14, 15]. Even for extremely large power flow loads, this approach consistently yields an accurate computation. The consequences of integrating a solar generator into the current network are the subject of the following phase of our inquiry.

This study describes a useful technique for determining power flow in radial networks. To test the accuracy and efficacy of the suggested technique on the simple and IEEE 33-bus radial distribution system, MATLAB simulations were carried out. A wide range of simulation results were examined to understand the effects of the addition of a renewable energy source such as the PV generator to the radial network. An ANN controller was used to determine the location of the PV generator that had already been integrated to the radial network. The outcomes of the identification process enhance the ANN controller's already outstanding efficacy and performance.

II. PV-RADIAL DISTRIBUTION NETWORK

Bus injection into the branch current matrix (BIBC) and analogous current injections are used to control the load flow of a radial distribution network [16]. This section explains the development process in detail. The corresponding current injection-based model is more useful for distribution networks. The complex apparent power load S_i for the buses is expressed as follows:

$$S_i = P_i + j.Q_i \quad (1)$$

where P_i and Q_i are the active and reactive load powers, respectively; and i is equal to 1, 2, 3, …, n.

The analogous current injection that corresponds to the *ii-th* solution iteration is:

$$I_i^{ii} = I_i^r(V_i^{ii}) + s.I_i^i(V_i^{ii}) = ((P_i + jQ_i)/V_i^{ii})* \quad (2)$$

where V_i^{ii} and I_i^{ii} represent the bus voltage and the equivalent current injection at the *ii-th* iteration and s^2 = -1. The corresponding current injection of the bus at the *ii-th* iteration is represented by the real and imaginary components I_i^r and I_i^i respectively.

A. Construction of Relationship Matrices

Figure 1 depicts a simple radial distribution network.

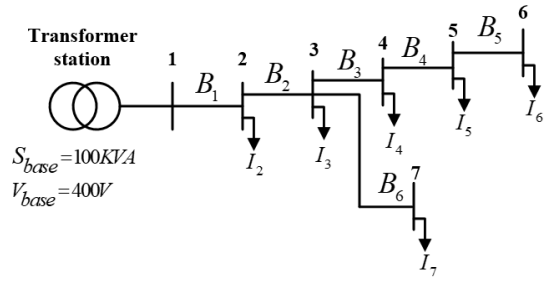

Fig. 1. Simple radial distribution network.

The injected currents are determined using (2). Kirchhoff's current law is used in the radial distribution network to determine the branch current. Thus, branch currents can be

formulated as functions of equivalent current injections. The branch currents B_1, B_2, B_3, B_4, B_5, and B_6 can be represented as:

$$\begin{cases} B_1 = I_2 + I_3 + I_4 + I_5 + I_6 + I_7 \\ B_2 = I_3 + I_4 + I_5 + I_6 + I_7 \\ B_3 = I_4 + I_5 + I_6 + I_7 \\ B_4 = I_5 + I_6 \\ B_5 = I_6 \\ B_6 = I_7 \end{cases} \quad (3)$$

Consequently, the connection between the branch currents and bus current injections can be described as:

$$\begin{bmatrix} B_1 \\ B_2 \\ B_3 \\ B_4 \\ B_5 \\ B_6 \end{bmatrix} = \begin{bmatrix} 1 & 1 & 1 & 1 & 1 & 1 \\ 0 & 1 & 1 & 1 & 1 & 1 \\ 0 & 0 & 1 & 1 & 1 & 0 \\ 0 & 0 & 0 & 1 & 1 & 0 \\ 0 & 0 & 0 & 0 & 1 & 0 \\ 0 & 0 & 0 & 0 & 0 & 1 \end{bmatrix} . \begin{bmatrix} I_1 \\ I_2 \\ I_3 \\ I_4 \\ I_5 \\ I_6 \end{bmatrix} \quad (4)$$

Equation (4) can be re-written as:

$$[B] = [BIBC].[I] \quad (5)$$

The branch injection to the branch current matrix is referred to as *BIBC*. The *BIBC* matrix only has the values 0 and 1, and it is an upper triangular matrix.

B. BIBC Matrices Development

The procedure for constructing the BIBC matrix presented in (4) is [15]:

- **Step 1:** The dimensions of the *BIBC* matrix for a distribution system with *m* branch sections and *n* buses are (*m, n -1*).
- **Step 2:** The column of the BIBC matrix's *i*-th bus should be copied to the column of the *j*-th bus if the line section B_{ii} lies between buses *i* and *j*. Subsequently, the locations of the *ii*-th row and *j*-th bus column should be filled with +1.
- **Step 3:** Repeat Step 2 until the *BIBC* matrix contains each line portion.

C. Bus Voltage Development

Using the generalized equations shown below, a forward sweep across the ladder network is used to determine the receiving-end bus voltages:

$$V(m2) = V(m1) - B(jj)\, Z(jj) \quad (6)$$

where *m1* and *m2* are the transmitting and receiving ends, respectively and *jj* and *B* represent the branch number and current, respectively.

Equation (7) can be used to determine the relationship between the branch currents and bus voltages.

$$\begin{cases} V_2 = V_1 - B_1 Z_{12} \\ V_3 = V_2 - B_2 Z_{23} \\ V_4 = V_3 - B_3 Z_{34} \\ V_5 = V_4 - B_4 Z_{45} \\ V_6 = V_5 - B_5 Z_{56} \\ V_7 = V_3 - B_6 Z_{37} \end{cases} \quad (7)$$

The following is the matrix representation for the aforementioned relations:

$$[\Delta V] = [BCBV].[B] \quad (8)$$

with:

$$[BCBV] = \begin{bmatrix} Z_{12} & 0 & 0 & 0 & 0 & 0 \\ Z_{12} & Z_{23} & 0 & 0 & 0 & 0 \\ Z_{12} & Z_{23} & Z_{34} & 0 & 0 & 0 \\ Z_{12} & Z_{23} & Z_{34} & Z_{45} & 0 & 0 \\ Z_{12} & Z_{23} & Z_{34} & Z_{45} & Z_{56} & 0 \\ Z_{12} & Z_{23} & 0 & 0 & 0 & Z_{37} \end{bmatrix}$$

Branch current variations cause equivalent bus voltage changes, which can be calculated using the *BCBV* matrix. The relationship between bus current injections and bus voltages can be expressed as follows.

$$[V] = [V_1] - [BCBV].[BIBC].[I] \quad (9)$$

The updated voltage values are used to perform a new top-down iteration. This process is repeated until the voltage levels in a row are within the permissible range.

Furthermore, branch *jj*'s actual and reactive power loss is provided by:

$$\begin{cases} p_{aloss} = \left|B(jj)^2\right| . \left|R(jj)\right| \\ q_{rloss} = \left|B(jj)^2\right| . \left|X(jj)\right| \end{cases} \quad (10)$$

D. PV Bus Development

Evidently, the ideal location for a PV source on a radial distribution line that is used to obtain the least amount of loss is at the end of the line. Equation (11) states the maximum power that a solar plant can supply [17]:

$$P_{GPV} = P_1 . E_c . \left[1 + P_2 . (E_c - E_{cref}) + P_3 . (T_{jc} - T_{jcref})\right] \quad (11)$$

where E_c corresponds to panel insolation (W/m^2), E_{cref} represents the reference insolation of 1000W/m^2, T_{jcref} denotes the reference panel temperature of 25°C, and parameters P_1, P_2, and P_3 have fixed values. With only 3 constant variables and a straightforward equation, this streamlined model allows the computation of the maximum power generated by a collection of panels for a specific panel illuminance and temperature.

Bus *i*'s active power changes with respect to:

$$P_{ci} = P_{ci0} - P_{GPV} \quad (12)$$

where P_{ci0} is the first power consumed before the PV generator is injected.

III. SIMULATION RESULTS AND DISCUSSION

A. Application on a Radial Distribution Test Network

We chose a 7-node radial distribution test network with 6 loads, 1 transformer station, and 6 lines for our study. Figure 2 shows the radial test network utilized. Note that the K_1 and K_2 switches are complementary.

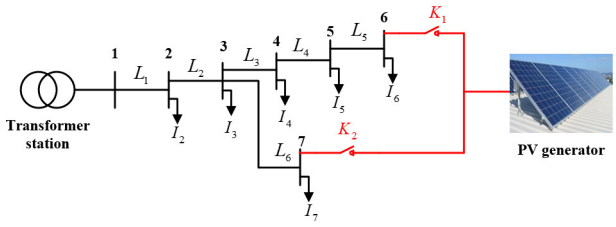

Fig. 2. Structure of the seven-node PV-radial distribution test network.

The line data and the data relating to the nodes are illustrated in Tables I and II, respectively.

TABLE I. LINE DATA

Number of the line	Liaison	Impedance (p.u.)
1	1-2	0.015 + j0.050
2	2-3	0.010 + j0.070
3	3-4	0.030 + j0.050
4	3-7	0.030 + j0.075
5	4-5	0.025 + j0.030
6	5-6	0.035 + j0.015

TABLE II. NODE DATA

Bus No	Types	Active power consumed (p.u.)	Reactive power consumed (p.u.)
1	P-V	0	0
2	P-Q	0.3	0.25
3	P-Q	0.4	0.15
4	P-Q	0.3	0.4
5	P-Q	0.7	0.45
6	P-Q	0.6	0.5
7	P-Q	0.5	0.7

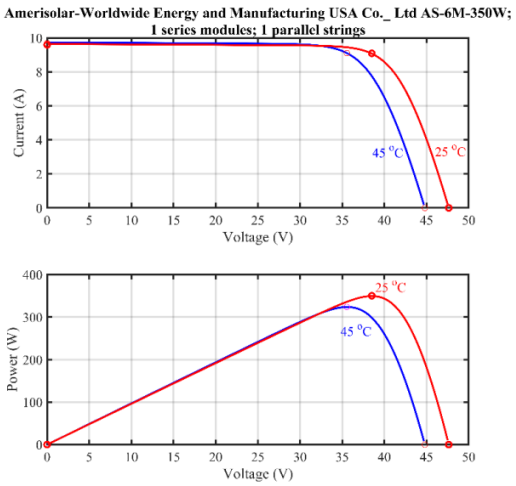

Fig. 3. PV module characteristics.

The Amerisolar-Worldwide Energy and Manufacturing USA Co._Ltd AS-6M-350W PV array type, shown in Figure 3, is suitable to perform the current requirements. The PV array parameters are reported in Table III.

TABLE III. PV MODULE PARAMETERS

Maximum power (W)	350
Voltage at MPP (V)	38.51
Current at MPP (A)	9.09
Open-circuit voltage (V)	38.51
Short-circuit current (A)	9.59

B. Simulation Results

In this study, two cases, with and without the PV generator (in node 6 or node 7) in the simple radial distribution network, were simulated and discussed. The *BIBC* matrix and equivalent current injection were used to determine the load flow in the radial distribution network. The load flow solution of a 7-bus distribution system for the radial network without the PV generator is summarized in Table V.

TABLE IV. LOAD FLOW SOLUTION OF THE RADIAL NETWORK

Bus N°	Voltage (p.u.)	Angle (rad.)
1	1.15	0
2	0.9769	–0.2306
3	0.9255	–0.6257
4	0.8986	–0.8477
5	0.8963	–0.9672
6	0.8748	–1.0186
7	0.8781	–0.7325

The radial distribution load flow had a total active power loss of 1.3924 p.u. and a total reactive power loss of 4.4914 p.u. Considering the case of an integrated PV generator in node 6 (case 01) or node 7 (case 02), Table IV illustrates the voltage solution of each bus with and without PV generator integration. Note that the PV generator power was set to 3.9 p.u.

TABLE V. LOAD FLOW SOLUTION WITH AND WITHOUT PV GENERATOR

	Voltage (p.u.)		
Bus N°	**Without**	**Case 01**	**Case 02**
1	1.15	1.15	1.15
2	0.9769	1.0584	1.0172
3	0.9255	0.9491	0.9087
4	0.8986	0.9877	0.8016
5	0.8963	1.0513	0.7598
6	0.8748	**1.1635**	0.7618
7	0.8781	0.8876	**1.2134**

Evidently from Table VI, the PV generator integration ensured a voltage increase in the node where the PV generator was integrated. In conclusion, after integrating a PV generator, the voltage modules were improved from different nodes. The most important voltages are those at which the PV generator is connected.

The branch currents for the two cases and the case without a PV generator are listed in Table VII. It is evident that the

injection of the PV generator increased the current magnitude of the branch where the PV generator was integrated. Moreover, the branch currents decreased, except for the nodes of the branches connected to the nodes where the PV generator was integrated. Figure 4 shows the active and reactive power losses for the case without a PV generator and for cases 01 and 02. Comparing these two cases with that without the PV generator, it is seen that the active and reactive power losses decreased after PV generator integration. Indeed, the power losses of case 01 were lower than those of case 02, indicating that the best integration node was node 6. In addition, the voltage plan of the case 01 was more reliable than that of case 02. The results were better for the most distant PV locations.

TABLE VI. BRANCH CURRENT MAGNITUDE SOLUTION OF THE PV-RADIAL NETWORK

	Branch current magnitude (p.u.)		
N°	**Without PV generator**	**Case 01**	**Case 02**
1	5.7284	2.4254	5.1432
2	5.3283	2.3567	5.1174
3	3.4965	2.3854	2.5879
4	2.7432	2.4689	1.9892
5	**1.3240**	**2.9720**	0.9786
6	**1.3280**	0.7605	**4.9831**

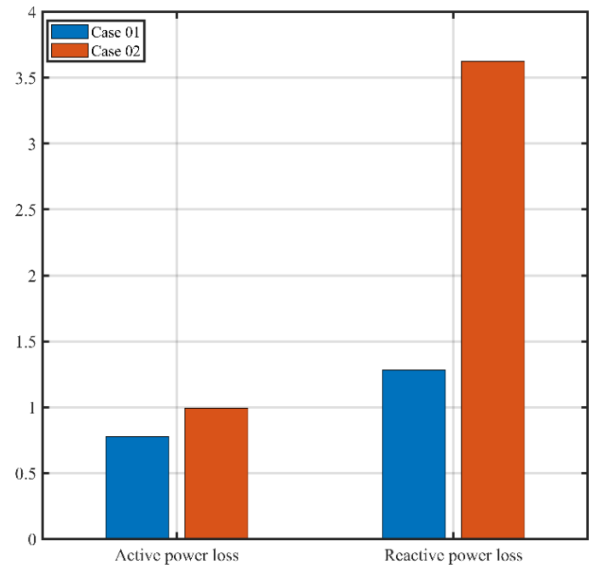

Fig. 4. Active and reactive power loss with and without PV generator.

TABLE VII. POWER LOSS SOLUTION OF THE PV-RADIAL NETWORK

Actual PV location nodes	**Active power loss (p.u.)**	**Reactive power loss (p.u.)**
02	1.3418	4.1688
03	0.9390	2.9652
04	3.3720	9.6416
05	0.9827	2.6175
06	0.7760	1.2828
07	0.9920	3.6237

To detect PV generator localization, an ANN control technique has been proposed [18, 19]. Table VIII lists the active and reactive power losses of the radial network system with respect to the node where the PV generator was injected. Figure 5 shows the ANN controller modeling design based on the data reported in Table VIII.

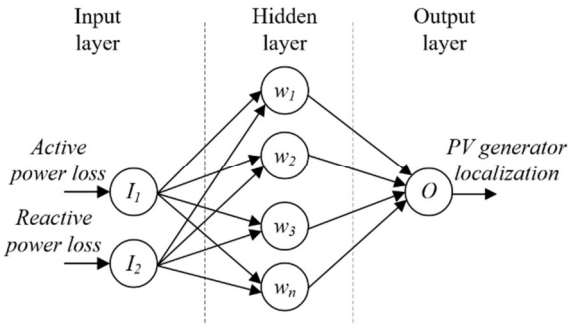

Fig. 5. ANN controller modeling design.

The MATLAB/Simulink environment was used to create the ANN model. Furthermore, the employed feedforward NN model had a hidden layer of 10 neurons, a hidden layer of 2 neurons, and an output layer of 1 neuron. A collection of localized PV generator data points based on simulations were trained using the Levenberg–Marquardt algorithm. The training performance curve demonstrates that the MSE error achieved at epoch 5 was 0.24085, as presented in Figure 6.

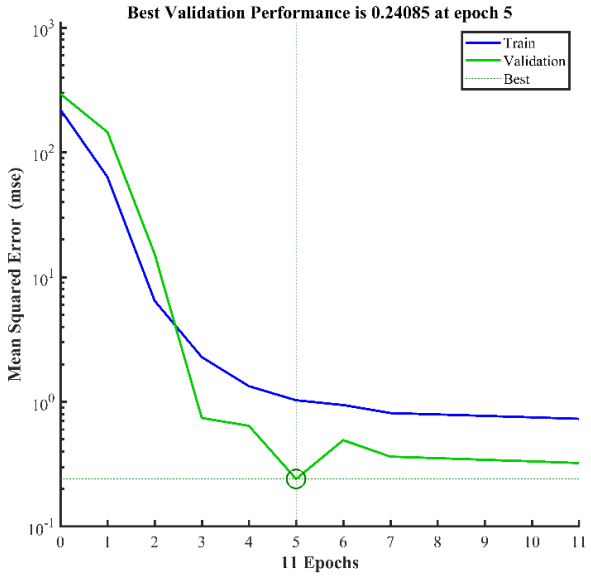

Fig. 6. ANN performance.

The best placement for the PV generator was determined by testing and verifying the 3 random values of the active and reactive power losses. The results of the identification procedure, which improves the efficacy and performance of the ANN controller, are displayed in Table IX.

TABLE VIII. ANN LOCALIZATION SOLUTION OF THE PV-RADIAL NETWORK

Active power loss (p.u.)	Reactive power loss (p.u.)	ANN localization
0.951	2.971	**04**
0.933	2.633	**05**
0.997	3.65	**07**

The proposed algorithm has also been implemented on the IEEE 33-bus radial distribution system with and without a PV Generator (PVG) as presented in Figure 7, to demonstrate its effectiveness. Thirty-three buses and 32 lines make up the system [20].

TABLE IX. LOAD FLOW SOLUTION OF THE IEEE 33-BUS RADIAL NETWORK WITHOUT PVG

Bus N°	Voltage (p.u.)	Angle (rad.)
1	1.0000000	0.0000000
2	0.9970252	0.0002549
3	0.9828930	0.0016899
4	0.9753834	0.0028438
5	0.9679571	0.0040162
6	0.9494792	0.0023728
7	0.9459544	-0.0016709
8	0.9322985	-0.0043500
9	0.9259658	-0.0056504
10	0.9200917	-0.0067634
11	0.9192229	-0.0066342
12	0.9177081	-0.0064295
13	0.9115324	-0.0080554
14	0.9092423	-0.0094567
15	0.9078155	-0.0101279
16	0.9064335	-0.0105421
17	0.9043854	-0.0119185
18	0.9037720	-0.0120894
19	0.9964968	0.0000658
20	0.9929192	-0.0011032
21	0.9922147	-0.0014411
22	0.9915772	-0.0017962
23	0.9793071	0.0011495
24	0.9726356	-0.0003994
25	0.9693105	-0.0011622
26	0.9475495	0.0030617
27	0.9449852	0.0040422
28	0.9335434	0.0054904
29	0.9253236	0.0068506
30	0.9217655	0.0086887
31	0.9176035	0.0072149
32	0.9166879	0.0068126
33	0.9164042	0.0066776

The load flow solution of an IEEE 33-bus distribution system for the radial network without PVG is illustrated in Table IX. Considering the case of an integrated PVG in nodes 1, 2...33, Table X illustrates the active and reactive power loss of each case.

Table XI represents the power loss solution of branches 15-16, 16-17, and 17-18. The GPV at node 16 supplies a significant portion of the energy from the GPV source installed at node 16. Additionally, nodes 17 and 18 in branches 15–16, 16–17, and 17–18 use the most energy. As you move away from node 16, the current in the branches decreases, which in turn causes the branches' losses to decrease. Thus, node 16, which has the lowest active and reactive losses, is the ideal position for the integration of the GPV.

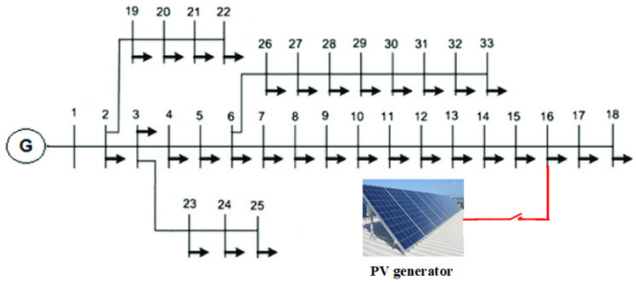

Fig. 7. Structure of the IEEE 33-bus radial distribution network with PVG.

TABLE X. POWER LOSS SOLUTION OF THE PVG- IEEE 33 BUS RADIAL NETWORK

Actual PVG location nodes	Active power loss (p.u.)	Reactive power loss (p.u.)
2	0.2093	0.1422
3	0.2014	0.1380
4	0.1973	0.1359
5	0.1932	0.1337
6	0.1843	0.1263
7	0.1832	0.1233
8	0.1762	0.1182
9	0.1731	0.1160
10	0.1703	0.1141
11	0.1699	0.1139
12	0.1692	0.1136
13	0.1667	0.1117
14	0.166	0.1109
15	0.1657	0.1106
16	**0.1655**	**0.1105**
17	0.1658	0.1108
18	0.1662	0.1111
19	0.2092	0.1420
20	0.20861	0.14151
21	0.20860	0.14150
22	0.2089	0.1419
23	0.1997	0.1369
24	0.1968	0.1346
25	0.1957	0.1338
26	0.1834	0.1258
27	0.1823	0.1252
28	0.1783	0.1218
29	0.1756	0.1195
30	0.1743	0.1188
31	0.1728	0.1175
32	0.1727	0.1173
33	0.1729	0.1177

Figure 8 illustrates the active and reactive power losses for the IEEE 33-bus network with PVG (01: injected in node 16) and without PVG (02). The reduction of active and reactive

losses in this study, when compared to previous works [21-21], is equal to 21.09% and 22.73%, respectively, as shown in Figure 8. This demonstrates the strong performance at this reduction level and even in the absence of shunt capacity, which lowers the cost of system installation. Additionally, compared to the other cases, the voltage plan for the case that integrated the PVG in node 16 was more reliable.

TABLE XI. BRANCH POWER LOSS SOLUTION OF THE PVG-IEEE 33 BUS RADIAL NETWORK

	Without PVG		With PVG (in node 16)	
Branch	**Active power loss (p.u.)**	**Reactive power loss (p.u.)**	**Active power loss (p.u.)**	**Reactive power loss (p.u.)**
15-16	0.287	0.210	**0.155**	**0.113**
16-17	0.257	0.343	**0.243**	**0.324**
17-18	0.054	0.043	**0.051**	**0.040**

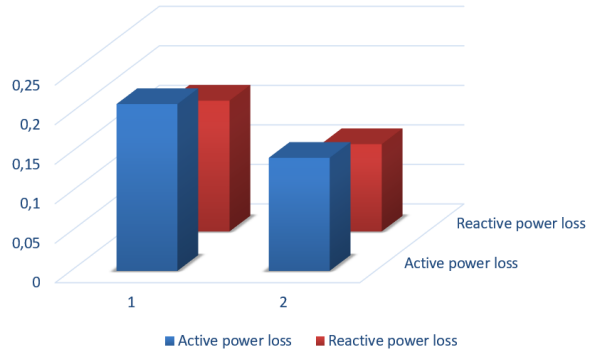

Fig. 8. Active and reactive power loss (1) without and (2) with PVG of the IEEE 33 bus network.

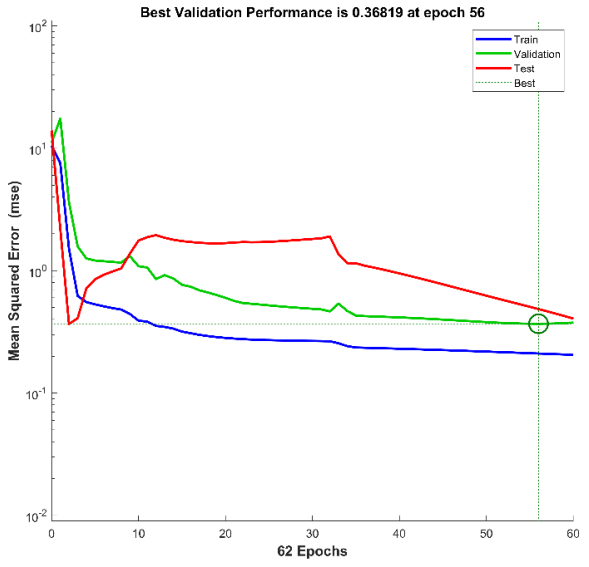

Fig. 9. IEEE 33-bus network ANN performance.

The Levenberg-Marquardt approach was used to train a set of localized PV generator data points based on simulations (Table XII). Thee representation of the training performance curve in Figure 9 shows that the obtained MSE at epoch 62 was 0.36819. The active and reactive power losses of 3 random variables were tested and verified to find the ideal location of the PV generator. The outcomes of the identification process, which enhances the ANN controller's effectiveness and performance, are shown in Table XIII.

TABLE XII. ANN LOCALIZATION SOLUTION OF THE PVG-IEEE 33-BUS RADIAL NETWORK

Active power loss (p.u.)	**Reactive power loss (p.u.)**	**ANN localization**
0.1168	0.1118	**13**
0.1996	0.1368	**23**
0.1759	0.1198	**30**

IV. CONCLUSION

In this study, an efficient technique for resolving the load flow radial distribution network problem was proposed. An ideal solution to the load flow issue was produced using two matrices generated from the topological properties of the distribution networks. The *BIBC* matrix was calculated based on Kirchhoff's current law. The *BCBV* matrix, which depicts the relationship between the bus voltages and branch currents, was used to resolve the load flow. These two matrices offer an easy methodology for handling load-flow problems when coupled. Consequently, the proposed method performed well in actual practice. Simulation results indicate that the proposed technique performs well for a widespread radial distribution network.

Owing to the developments in renewable energy sources, PV generators have been integrated into the radial system under study. To obtain the best location for a PV generator, the simulation results regarding the voltage amplitudes, current branches, and active and reactive power losses were presented and discussed in this paper. Based on these results, the best location to integrate a PV generator was determined as the farthest node, which provides reliable voltage and less power loss. In addition, to locate a PV generator that was already integrated into the radial network, an ANN controller was applied. The results of the identification procedure improved the efficacy and performance of the ANN controller.

ACKNOWLEDGMENT

The authors would like to thank Editage for English language editing.

REFERENCES

[1] T. Le and B. L. N. Phung, "Load Shedding in Microgrids with Consideration of Voltage Quality Improvement," *Engineering, Technology & Applied Science Research*, vol. 11, no. 1, pp. 6680–6686, Feb. 2021, https://doi.org/10.48084/etasr.3931.

[2] M. A. Zdiri, A. S. Alshammari, A. A. Alzamil, M. B. Ammar, and H. H. Abdallah, "Optimal Shedding Against Voltage Collapse Based on Genetic Algorithm," *Engineering, Technology & Applied Science Research*, vol. 11, no. 5, pp. 7695–7701, Oct. 2021, https://doi.org/10.48084/etasr.4448.

[3] C. Seneviratne and C. Ozansoy, "Frequency response due to a large generator loss with the increasing penetration of wind/PV generation – A literature review," *Renewable and Sustainable Energy Reviews*, vol. 57, pp. 659–668, May 2016, https://doi.org/10.1016/j.rser.2015.12.051.

[4] M. C. Herrera-Briñez, O. D. Montoya, L. Alvarado-Barrios, and H. R. Chamorro, "The Equivalence between Successive Approximations and Matricial Load Flow Formulations," *Applied Sciences*, vol. 11, no. 7, Jan. 2021, Art. no. 2905, https://doi.org/10.3390/app11072905.

[5] T. Shen, Y. Li, and J. Xiang, "A Graph-Based Power Flow Method for Balanced Distribution Systems," *Energies*, vol. 11, no. 3, Mar. 2018, Art. no. 511, https://doi.org/10.3390/en11030511.

[6] O. D. Montoya and W. Gil-González, "On the numerical analysis based on successive approximations for power flow problems in AC distribution systems," *Electric Power Systems Research*, vol. 187, Art. no. 106454, Oct. 2020, https://doi.org/10.1016/j.epsr.2020.106454.

[7] O. D. Montoya, W. Gil-González, and D. A. Giral, "On the Matricial Formulation of Iterative Sweep Power Flow for Radial and Meshed Distribution Networks with Guarantee of Convergence," *Applied Sciences*, vol. 10, no. 17, Art. no. 5802, Jan. 2020, https://doi.org/10.3390/app10175802.

[8] O. D. Montoya, L. E. Rueda, W. Gil-González, A. Molina-Cabrera, H. R. Chamorro, and M. Soleimani, "On the Power Flow Solution in AC Distribution Networks Using the Laurent's Series Expansion," in *2021 IEEE Texas Power and Energy Conference (TPEC)*, Oct. 2021, pp. 1–5, https://doi.org/10.1109/TPEC51183.2021.9384936.

[9] B. Sereeter, A. S. Markensteijn, M. E. Kootte, and C. Vuik, "A novel linearized power flow approach for transmission and distribution networks," *Journal of Computational and Applied Mathematics*, vol. 394, Art. no. 113572, Oct. 2021, https://doi.org/10.1016/j.cam.2021.113572.

[10] K. Anoune, M. Bouya, A. Astito, and A. B. Abdellah, "Sizing methods and optimization techniques for PV-wind based hybrid renewable energy system: A review," *Renewable and Sustainable Energy Reviews*, vol. 93, pp. 652–673, Oct. 2018, https://doi.org/10.1016/j.rser.2018.05.032.

[11] M. Zangiabadi, R. Feuillet, and H. Lesani, "An approach to deterministic and stochastic evaluation of the uncertainties in distributed generation systems," in *CIRED 2009 - 20th International Conference and Exhibition on Electricity Distribution - Part 1*, Prague, Czech Republic, Jun. 2009, pp. 1–4, https://doi.org/10.1049/cp.2009.1098.

[12] D. R. H. Al-Rubayi and A. M. Alrawi, "Optimal Size and Location of Distributed Generators using Intelligent Techniques," *Engineering And Technology Journal*, vol. 28, no. 23, pp. 6623–6633, 2010.

[13] M. Akorede, H. Hizam, I. Aris, and Z. Kadir, "A Review of Strategies for Optimal Placement of Distributed Generation in Power Distribution Systems," *Research Journal of Applied Sciences*, vol. 5, no. 2, pp. 137–145, Feb. 2010, https://doi.org/10.3923/rjasci.2010.137.145.

[14] M. A. Mates, "A new power flow method for radial networks," in *2003 IEEE Bologna Power Tech Conference Proceedings,* Bologna, Italy, Jun. 2003, vol. 2, https://doi.org/10.1109/PTC.2003.1304335.

[15] J.-H. Teng, "A direct approach for distribution system load flow solutions," *IEEE Transactions on Power Delivery*, vol. 18, no. 3, pp. 882–887, Jul. 2003, https://doi.org/10.1109/TPWRD.2003.813818.

[16] S. Sivanagaraju, J. Viswanatha Rao, and M. Giridhar, "A loop based load flow method for weakly meshed distribution network," *ARPN Journal of Engineering and Applied Sciences*, vol. 3, no. 4, pp. 55–59, Jan. 2008.

[17] D. Rekioua and S. Aissou, "Photovoltaic Panels Characteristics Methods," in *Proceedings Engineering & Technology*, Jan. 2013, vol. 1, pp. 68–174.

[18] M. A. Zdiri *et al.*, "Design and Analysis of Sliding-Mode Artificial Neural Network Control Strategy for Hybrid PV-Battery-Supercapacitor System," *Energies*, vol. 15, no. 11, p. 4099, Jan. 2022, https://doi.org/10.3390/en15114099.

[19] J. Chakravorty, S. Shah, and H. N. Nagraja, "ANN and ANFIS for Short Term Load Forecasting," *Engineering, Technology & Applied Science Research*, vol. 8, no. 2, pp. 2818–2820, Apr. 2018, https://doi.org/10.48084/etasr.1968.

[20] V. Vita, "Development of a Decision-Making Algorithm for the Optimum Size and Placement of Distributed Generation Units in Distribution Networks," *Energies*, vol. 10, no. 9, Sep. 2017, Art. no. 1433, https://doi.org/10.3390/en10091433.

[21] M. Dixit, P. Kundu, and H. R. Jariwala, "Incorporation of distributed generation and shunt capacitor in radial distribution system for techno-economic benefits," *Engineering Science and Technology, an International Journal*, vol. 20, no. 2, pp. 482–493, Apr. 2017, https://doi.org/10.1016/j.jestch.2017.01.003.